Impact of Extended π Conjugation on Methyl Rotor-Induced IVR in Aromatic Molecules

Partha Biswas, Sujit S. Panja, S. Manogaran, and Tapas Chakraborty*

Department of Chemistry, Indian Institute of Technology Kanpur, UP 208016 India

Received: October 10, 2004; In Final Form: February 14, 2005

Laser-induced fluorescence excitation and resolved fluorescence spectra following excitations of the single vibronic levels (SVL) of *p*-vinyltoluene (*p*-VT) and *p*-vinylfluorobenzene (*p*-VFB) have been measured in a seeded supersonic free-jet expansion. A complete vibronic assignment of the fluorescence spectrum measured following excitation of the 0_0^0-band of *p*-VT has been presented. Normal vibrational modes in the S_0 and S_1 states of the molecule have been calculated by CASSCF method, and the correlation between the two set of modes is made by expressing the excited-state normal modes in terms of those of the ground state. The calculations predict that in the excited state methyl and vinyl torsional motions of *p*-VT are extensively mixed with many of the out-of-plane modes of the aromatic ring. Our resolved fluorescence spectral data measured following SVL excitations essentially agree with such predictions. In the excited state, the molecule exhibits a dramatically low threshold for the rotor-induced IVR in a supersonic jet expansion. Several mechanisms have been discussed to explain the phenomenon.

I. Introduction

The possibility that the internal rotational motion of the methyl group can accelerate IVR in a polyatomic molecule has been discussed over the past two decades.[1−21] Parmenter and Stone were the first to present evidences for this phenomenon by comparing the fluorescence spectra of *p*-fluorotoluene (*p*-FT) and *p*-difluorobenzene (*p*-DFB) vapors in a bulb at 300 K.[1] The IVR threshold in *p*-FT was found to be much lower compared to that in *p*-DFB, and the same was manifested also in their chemical timing studies.[3] However, this spectral manifestation of the excited-state behavior of *p*-FT disappears when the supersonic jet-cooled samples were used. A much slower IVR rate of the molecule was noticed also in a time-resolved measurement in a supersonic molecular beam[4] compared to the rates estimated in chemical timing studies in a bulb.

In this article, we demonstrate that the threshold for the rotor-induced vibronic level mixing in rotationally and vibrationally cold aromatic samples in the excited state can be dramatically lowered by chemical modification of the π-characteristics of the aromatic ring. A vinyl substitution at the para position of toluene, which does not introduce any additional steric crowding for internal rotation of the $-CH_3$ group at the other end of the ring (Figure 1), has been found to have the required attributes to stimulate the effect. In an analogous case of *p*-aminotoluene, Yan and Spangler showed earlier that the methyl torsion effectively couples with the large amplitude amine inversion in the S_1 state.[7] The signature of such coupling is manifested in the fluorescence excitation spectrum as the splitting of the amine overtone band into several components. The observations were explained in terms of hyperconjugation. To our knowledge, the effects of such coupling in resolved fluorescence spectra following single vibronic level (SVL) excitations have not been investigated. We show here that, unlike *p*-aminotoluene, the coupling of the methyl torsion with other large amplitude motions is not directly manifested in the absorption spectrum.

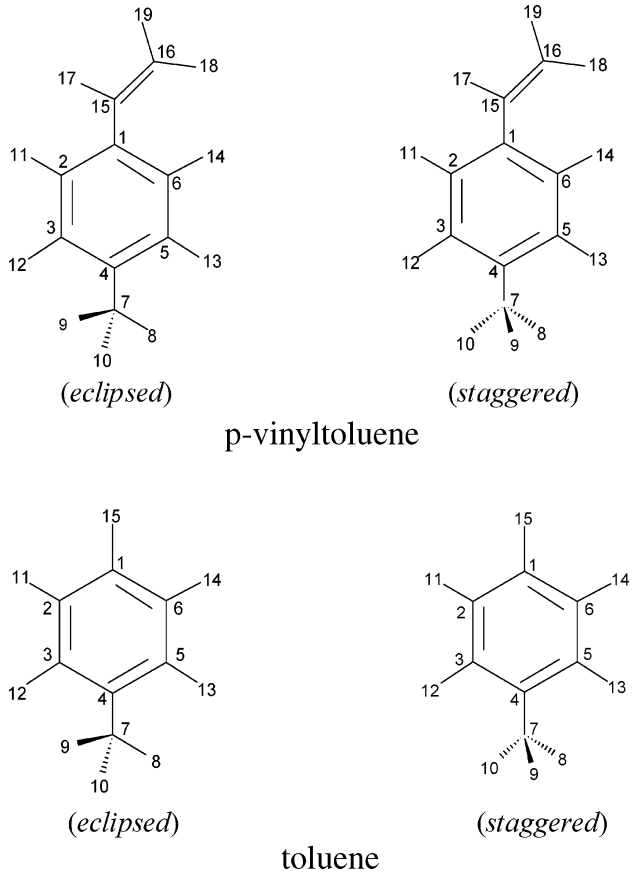

Figure 1. Atom numbering scheme used for geometry optimization of *p*-VT, T, and *p*-FT in their staggered and eclipsed conformations.

However, the resolved fluorescence spectra measured following excitations of several vibronic bands reveal that the methyl torsion is mixed with many of the other vibrational modes in the excited-state mediated by the large amplitude torsional motion of the vinyl group, through a chain of coupling process. Theoretical calculations at various levels for the ground as well

* To whom correspondence should be addressed. Phone: 91 512 2597772. Fax: 91 512 2597436. E-mail: tapasc@iitk.ac.in.

10.1021/jp045383s CCC: $30.25
Published on Web 03/17/2005

TABLE 1: Geometrical Parameters of *p*-VT in S_0 and S_1 States for the Eclipsed and Staggered Conformations of the Methyl Group, Predicted by the HF, MP2, CASSCF, and CIS Calculations using the 6-311G Basis Set[a]**

energy and parameters	ground state									excited state					
	HF			MP2			CASSCF			CIS			CASSCF		
	eclp.	stag.	(Δ)	eclp.	stag.	(Δ)	eclp.	stag.	(Δ)	eclp.	stag.	(Δ)	eclp.	stag.	(Δ)
relative energy (cm-1)	0	−19.6		0	−31.9		0	−16.7		0	−15.9		0	−18.9	
C_1-C_2	1.391	1.389	−0.002	1.407	1.406	−0.001	1.401	1.399	−0.002	1.434	1.436	0.002	1.443	1.444	0.001
C_2-C_3	1.383	1.385	0.002	1.395	1.397	0.002	1.392	1.395	0.003	1.354	1.355	0.001	1.430	1.429	−0.001
C_3-C_4	1.388	1.385	−0.003	1.403	1.402	−0.001	1.398	1.395	−0.003	1.442	1.438	−0.004	1.428	1.430	0.002
C_4-C_5	1.389	1.392	−0.003	1.403	1.405	0.002	1.398	1.401	0.003	1.392	1.395	0.003	1.430	1.429	−0.001
C_5-C_6	1.382	1.379	−0.003	1.396	1.394	−0.002	1.392	1.390	−0.002	1.375	1.373	−0.002	1.434	1.436	0.002
C_1-C_6	1.391	1.394	0.003	1.406	1.407	0.001	1.402	1.404	0.002	1.463	1.463	0.00	1.437	1.439	0.002
C_4-C_7	1.510	1.510	0.00	1.509	1.508	−0.001	1.511	1.511	0.00	1.496	1.499	0.003	1.504	1.504	0.00
$C_7\cdots H_{13}$	2.732	2.723	−0.009	2.742	2.734	−0.008	2.742	2.733	−0.009	2.731	2.720	−0.011	2.765	2.753	−0.012
$C_5\cdots H_8$	2.634			2.639			2.642			2.647			2.654		
$H_8\cdots H_{13}$	2.385			2.383			2.395			2.396			2.414		
$\angle C_4$-C_7-H_8	111.2	111.2	0.00	111.1	111.0	−0.10	111.2	110.9	−0.30	111.7	111.2	−0.50	111.4	111.2	−0.20
$\angle C_5$-C_4-C_7	121.5	121.0	−0.50	121.4	120.9	−0.50	121.6	121.0	−0.60	122.4	121.6	−0.80	121.5	120.8	−0.70
$\angle C_3$-C_4-C_5	117.7	117.7	117.7	0.00	117.9	0.00	117.7	117.7	0.00	118.4	118.3	−0.10	118.2	118.2	0.00

[a] The differences in geometrical parameters (Δ) for the two conformations are also presented. All distances are in angstrom and angles in degree units.

as excited electronic states have been carried out to interpret the experimental results.

II. Methods

A. Experiment. The experimental setup used to measure the laser-induced fluorescence excitation and dispersed fluorescence spectra has been described previously.[22,23] Briefly, the *p*-vinyltoluene and *p*-vinylfluorobenzene vapors are mixed with helium at a pressure of 2 atm and expanded into vacuum through a pulsed nozzle (General Valve) of orifice diameter 0.5 mm to generate a supersonic free jet. The jet-cooled molecules were excited by a tunable UV laser obtained as the doubled output of a dye laser (Sirah and Plasma Technik, model: Cobra Stretch) pumped by the second harmonic of a Nd:YAG laser (Spectra Physics, model: INDI). To measure the dispersed fluorescence spectra, a 0.75 m monochromator (Spex, model 750M) with a grating of groove density of 2400/mm was used to disperse the fluorescence before detection. Typical spectral resolution of the results presented here is 7 cm^{-1}. The fluorescence was detected using a Hamamatsu R928 photomultiplier tube and the output signal of the photomultiplier was processed by a boxcar averager (SRS 250) and the data were stored in a personal computer.

The samples *p*-vinyltoluene and *p*-vinylfluorobenzene were procured from Lancaster and purified further by vacuum distillation.

B. Calculations. The ground-state geometries of all of the molecules are optimized at the HF, MP2, and CASSCF levels of theory using the 6-311G** basis set, and for the excited state (S_1), the CIS and CASSCF methods have been used with the same basis set. For CASSCF calculations, the active spaces are comprised of eight π electrons and eight π and π^* orbitals for *p*-VT, and six π electrons and six π and π^* orbitals for toluene and *p*-fluorotoluene. Vibrational frequencies (in harmonic approximation) in the ground as well as in the excited states are calculated by the CASSCF method using 6-31G* basis set. Ground-state normal-mode frequencies are also calculated by the DFT method using the Becke3LYP functional with 6-311G** basis set. All calculations are carried out using the G-98 suite of program.[26]

III. Results and Discussion

A. Quantum Chemistry Calculations. *A.1. Molecular Geometry.* The theoretically predicted geometrical parameters of *p*-VT for the eclipsed and staggered conformations of the methyl group in the ground (S_0) and first excited (S_1) electronic states are presented in Table 1. In both the states the vinyl group is nearly coplanar with the aromatic ring, and the staggered geometry is slightly more stable than the eclipsed. The energy differences between the two conformations in the ground state are 20, 17, and 32 cm^{-1} according to the predictions of the HF/6-311G**, CASSCF/6-311G**, and MP2/6-311G** levels of calculations, respectively. In the excited state, the energy differences are 16 and 19 cm^{-1} at the CIS/6-311G** and CASSCF/6-311G** calculations, respectively. The CASSCF predicted relative energies of the conformers are very close to those estimated experimentally by Hollas et al. (discussed later).

The data in the Table 1 show that, in the ground state, different C−C bond lengths of the phenyl ring are predicted somewhat smaller (∼0.01 Å) at the HF level compared to those by MP2 and CASSCF calculations. Likewise, in the excited state, those parameters predicted at the CIS level are relatively smaller by the same extent compared to the CASSCF values. The high-resolution spectroscopy studies of several substituted benzenes have indicated that $S_1 \leftarrow S_0$ electronic excitation causes a little expansion of the aromatic ring.[13,27] The results of CASSCF calculations of the present study predict the same behavior. The CIS as well as CASSCF data predict that the ring geometry in the excited state is almost insensitive to the conformational state of the methyl group (staggered vs eclipsed). However, the $C_7\cdots H_{13}$ nonbonded distance and $\angle C_5-C_4-C_7$ bond angle are somewhat larger in the eclipsed geometry in both the electronic states. For example, in the ground state, the two parameters are 0.009 Å and 0.6° larger in the eclipsed than the staggered according to the predictions of CASSCF calculations, and in the excited state, these differences are 0.012 Å and 0.7°, respectively. Furthermore, there occurs a 0.007 Å shortening of the bond length between the methyl group and ring (C_4-C_7) in S_1 compared to S_0. Obviously, there is steric interaction between the methyl group and the ortho hydrogen atoms of the aromatic ring in the eclipsed geometry and which is responsible for a finite torsional barrier. However, the important point of the theoretical prediction concerning the present study is that such interactions do not affect the ring geometry.

In Table 2, we have shown comparisons of a few selected geometrical parameters of *p*-VT with those of toluene and *p*-FT

TABLE 2: Comparison of Selected Geometrical Parameters for the Eclipsed Conformation of *p*-Vinyltoluene with Theose of Toluene and *p*-Fluorotoluene Predicted by CASSCF/6-311G(d,p) Calculations in S_0 and S_1 Electronic States

	ground state			excited state		
geometrical	*p*-vinyl toluene	*p*-fluoro toluene[a]	toluene	*p*-vinyl toluene	*p*-fluoro toluene[a]	toluene
C_1-C_2 (Å)	1.401	1.386	1.392	1.443	1.419	1.432
C_2-C_3 (Å)	1.392	1.392	1.397	1.430	1.434	1.432
C_3-C_4 (Å)	1.398	1.402	1.396	1.428	1.440	1.438
C_4-C_5 (Å)	1.398	1.396	1.402	1.430	1.441	1.437
C_5-C_6 (Å)	1.392	1.397	1.392	1.434	1.441	1.435
C_1-C_6 (Å)	1.402	1.381	1.396	1.437	1.419	1.431
C_4-C_7 (Å)	1.511	1.511	1.511	1.504	1.504	1.504
$H_8\cdots H_{13}$ (Å)	2.395	2.391	2.389	2.414	2.413	2.418
$C_5\cdots H_8$ (Å)	2.642	2.637	2.638	2.654	2.650	2.655
$C_7\cdots H_{13}$ (Å)	2.742	2.740	2.737	2.765	2.768	2.772
$\angle C_4-C_7-H_8$ (degree)	111.2	111.2	111.3	111.4	111.5	111.4
$\angle C_5-C_4-C_7$ (degree)	121.6	121.4	121.4	121.5	120.9	121.3
$\angle C_3-C_4-C_5$ (degree)	117.7	118.2	118.3	118.2	119.5	118.7

[a] Atom numbering is same as that of *p*-VT and toluene.

in the S_0 as well as S_1 states. The nonbonding distances $H_8\cdots H_{13}$, $C_5\cdots H_8$, and $C_7\cdots H_{13}$ in the ground state are a little longer in *p*-VT compared to those in the other two molecules. In the excited state (S_1), these nonbonding distances are increased along with the C−C bond lengths of the aromatic ring. It is noteworthy that the largest increments of these parameters occur in toluene and the least in *p*-VT. This would imply that, on electronic excitation from S_0 to S_1, the van der Waals interactions between the methyl group and phenyl ring are altered to the smallest extent in *p*-VT than in the two other molecules. Another important parameter concerning the van der Waals intercation is the C−C bond length between the methyl group and the phenyl ring. It is smaller in S_1 compared to S_0, but the changes are predicted to be the same in all three molecules.

A.2. Normal Vibrations in S_0 and S_1. The vibrational frequencies (in harmonic approximation) and brief descriptions of the normal modes for the staggered conformation of *p*-VT calculated at the CASSCF/6-31G* level in both the S_0 and S_1 states are presented in Table 3. The vibrations are classified and numbered according to in-plane and out-of-plane atomic motions. Considering an approximate planar C_s symmetry point group, the in-plane and out-of-plane vibrations of the molecule transform to a′ and a″ representations, respectively. A comparison between the gas-phase IR absorption spectrum[32] and resolved fluorescence spectrum from the 0^0 level of the S_1 state of the jet-cooled molecules (presented below, Figure 5) indicates that the vibrational features are mutually exclusive in the two spectra. The IR spectrum shows transitions to vibrational levels which are not accessible by electronic transition from the 0^0 level of S_1 and vice versa. The vibrational frequencies and IR transition intensities calculated at the DFT/B3LYP/6-311G** level are in reasonable agreement with the observations.

The CASSCF calculation predicts that the methyl and vinyl torsional frequencies in the ground state of *p*-VT are 15 and 12 cm^{-1}, respectively. However, the experimentally measured frequency for the latter is 38 cm^{-1} in vinylbenzene (styrene) and 36 cm^{-1} in *p*-vinylfluorobenzene (4-fluorostyrene).[33] Thus, the calculated frequency of this large amplitude mode seems to be unreliable at this level. On the other hand, the frequencies predicted by the DFT method for the two modes are 21 and 72 cm^{-1}, respectively. Therefore, we have designated the vinyl torsion as the mode number 50 (Table 3) and methyl torsion as the mode 51. One apparent reason for the large variations in predicted frequencies for the vinyl torsion at different levels of theoretical calculations is because of a highly flat-bottomed potential energy curve for the mode in the ground state. The predicted frequencies for other modes obtained by the two theoretical methods (CASSCF and DFT) are found comparable.

Visualization of the atom displacement vectors of the normal modes indicate that the one-to-one correlation between the ground and excited state vibrations are reasonably maintained for the high-frequency C−H stretching and in-plane ring modes, but the out-of-plane vibrations exhibit large alterations in mode characteristics. In the case of styrene, strong Duschinsky mixing was proposed for some modes, wherein a given excited state mode may correlate with several ground state modes, and the point has been discussed extensively by Hemley et al.[31] In the present case, to get theoretical predictions of such mode mixing, the excited-state normal modes are expanded on the basis of the ground-state modes (Table 4). The results show that the excited states mode 51 (Q'_{51}) looks dominantly methyl torsion (Q''_{51}) type, mixed with a small fraction of vinyl torsion (Q''_{50}). However, Q'_{50} appears almost equal proportions of Q''_{50} and Q''_{49} (out-of-plane vinyl bending) with some contribution from Q''_{51}. Likewise, the mode 49 (Q'_{49}) in S_1 is transformed to the methyl torsion (Q''_{51}), vinyl torsion (Q''_{50}), vinyl bending (Q''_{49} and Q''_{48}), and out-of-plane plane ring puckering modes (Q''_{47}). The mode Q'_{48} is mostly similar to Q''_{48} (out-of-plane bending of vinyl and methyl group), but small contributions of the two out-of-plane ring puckering vibrations (Q''_{46} and Q''_{47}) are there along with the vinyl torsion (Q''_{50}). Hollas et al predicted strong Duschinsky mixing between the vinyl torsion and vinyl bending vibrations in the S_1 surface of styrene.[33] The present theoretical study on *p*-VT predicts that a *para* methyl substitution expands the mixing space. The rotor mode induces mixing of many of the out-of-plane modes, and a such process can profoundly affect the dynamics of the molecule in the excited-state surface.[38] The atomic displacement vectors of a few ring modes, which are predicted to undergo mixing with the methyl and vinyl torsions and vinyl bending in the S_1 state, are presented in Figure 2.

B. Fluorescence Excitation Spectra. The laser-induced fluorescence excitation (FE) spectrum for $S_1 \leftarrow S_0$ excitation of *p*-VT measured in a supersonic free jet expansion of helium is presented in Figure 3. The spectrum shows a number of low-frequency vibronic features (18, 33, and 53 cm^{-1}) near the origin. Hollas et al. assigned these bands to torsional excitations of the methyl group. To depict the effect of π conjugation of the *p*-vinyl group on vibronic activities of torsional transitions in this spectrum, the features of the $S_1 \leftarrow S_0$ spectrum of toluene measured by Hickman et al.[25] are presented here for a comparison in the stick spectral format (Figure 3b). The spectrum contains only one weak low-frequency band at 55

TABLE 3: Normal Mode Vibrational Frequencies in the S_0 and S_1 States along with Their Approximate Mode Descriptions Calculated at the CASSCF/6-31G* Level[a]

	ground state (S_0)		excited state (S_1)	
mode no.	frequency (cm^{-1})	brief description	frequency (cm^{-1})	brief description
1	3418	vinyl νCH	3429	vinyl νCH
2	3380	ring CH	3406	ring νCH
3	3364	ring νCH	3384	ring νCH
4	3347	ring νCH	3370	ring νCH
5	3344	ring νCH	3366	ring νCH
6	3341	vinyl νCH + ring νCH	3346	vinyl νCH + ring νCH
7	3326	vinyl νCH	3326	vinyl νCH
8	3276	νCH in CH_3	3270	νCH in CH_3
9	3257	νCH in CH_3	3244	νCH in CH_3
10	3202	νCH in CH_3	3190	νCH in CH_3
11	1783	vinyl (βCH+ νCC) + ring νCC	1847	ring νCC
12	1765	ring (νCC + βCH)	1710	ring (νCC+βCH)
13	1708	ring (νCC + βCH)	1687	vinyl (νCC+βCH)
14	1670	ring CH + ring α	1605	ring(νCC+βCH)+vinyl βCH
15	1587	vinyl βCH($=CH_2$ scissor)	1578	ring βCH
16	1537	ring βCH	1552	vinyl βCH + aryl βCH
17	1459	ring βCH+ vinyl β($CH=CH_2$)	1442	ring βCH
18	1426	vinyl βCH+ vinyl νCC	1413	ring βCH
19	1334	aryl CH + α ring	1364	vinyl (νCC+βCH)
20	1305	aryl βCH + ring νCC	1293	aryl βCH + aryl α(C−C−C)
21	1296	aryl βCH	1276	aryl βCH
22	1269	ring νCC + ring deform	1254	aryl βCH + $\nu(C_1-C_\alpha)$
23	1188	ring νCC + ring βCH	1168	aryl βCH + CH bending in CH_3
24	1147	C−H bending in CH_3	1119	CH bending in CH_3
25	1131	vinyl βCH	1116	vinyl βCH + CH bending in CH_3
26	1103	aryl βCH + ring deform	1011	aryl βCH + aryl βCC
27	1077	CH bend in CH_3	1008	aryl βCH + CH bending in CH_3
28	869	ring breathing	816	ring breathing
29	752	vinyl β at C_α + aryl-CH_3 bend	742	νC−CH_3+ vinyl βCH + aryl βCH
30	692	ring αC−C−C (6*b*type)	627	aryl _C−C−C (6*b*type)
31	563	vinyl β at Cα + α ring	551	vinyl βC_α
32	441	ring αC−C−C (4*a* type)	409	ring deform (4*a*type)
33	365	vinyl β at C1+ CH_3 bending	353	vinyl βat C1+ βCH_3
34	221	vinyl β at C1	219	vinyl β at C1
35	1637	CH bending in CH_3	1639	CH bending in CH_3
36	1636	scissoring in CH_3	1633	scissoring in CH_3
37	1569	CH_3 inversion	1567	CH_3 inversion
38	1046	vinyl γCH	1016	vinyl γCH
39	987	aryl γCH	786	vinyl γ-terminal CH_2
40	983	aryl γCH	697	aryl γCH
41	864	aryl γCH	677	aryl γCH
42	858	vinyl γ-terminal CH_2	667	aryl γCH + vinyl CH_2 twist
43	850	aryl γCH + vinyl γCH	593	aryl γCH + vinyl γCH
44	759	ring puckering	576	aryl γCH
45	652	ring puckering + vinyl γCH	508	ring pucker (4 type) + vinyl γCH
46	486	γring (16*b* type) + vinyl γCH	394	ring pucker (6*b* type) + vinyl twist
47	431	γ ring (16*a* type)	292	ring pucker (6*a* type)
48	305	γ_{vinyl} + γCH_3 + ring puckering	244	γ_{vinyl} + γCH_3 + ring puckering
49	141	γ_{vinyl} + γCH_3	161	vinyl torsion
50	12	γvinyl	77	γ_{vinyl} + γCH_3
51	15	CH_3 torsion	57	CH_3 torsion

[a] ν, stretching; α, in-plane ring angle bend; β, in-plane bend; γ, out-of-plane bend.

cm^{-1}, and it was assigned as $0a' \rightarrow 3a''$ transition of the methyl rotor, and this is in contrast to the pronounced activities of the torsional vibronic transitions in the former. The FE spectrum of *p*-FT was measured and analyzed by Okuyama et al.[34] and Zhao et al.,[28] and in both cases the vibronic transitions corresponding to the methyl rotor are very weak compared to the electronic origin band. These comparisons indicate that *p*-vinyl substitution of the toluene ring enhances the intensities of the vibronic bands of the methyl torsional mode.

The other vibronic bands beyond 214 cm^{-1} in this spectrum are likely to represent the modes involving the aromatic ring and vinyl group. As mentioned before, only the in-plane modes of a′ symmetry and overtones and totally symmetric combinations of the out-plane modes are expected to show up in the excitation spectrum from the zero-point level in S_0. The actual mode characteristics of the observed bands are discussed later. Here, to see to what extent these relatively higher frequency transitions bear the influence of the rotor, the FE spectrum of an analogous molecule, but without a rotor group, *p*-vinylfluorobenzene (*p*-VFB), has been measured and presented (Figure 3c) for comparison. The spectrum is identical to the mass-selected REMPI spectrum of the molecule measured recently by Georgiev et al.[24] A comparison between parts a and c of Figure 3 shows that, except the low-frequency features in the former, the band structures beyond 200 cm^{-1} are quite similar in the two spectra. This indicates that the higher frequency vibronic bands in the FE spectrum of *p*-VT originate primarily from the vinylbenzene chromophore.

A notable characteristic of the FE spectral feature of *p*-VT is that the low-frequency rotor progression does not build up

TABLE 4: Excited State normal Modes in Terms of Ground State normal Modes of p-VT in Staggered Conformation[a]

S_1modes	expansion in S_0 modes
Q_1'	$= 0.993\ Q_1'' - 0.117\ Q_2''$
Q_2'	$= -0.117\ Q_1'' - 0.988\ Q_2''$
Q_3'	$= 0.991\ Q_3''$
Q_4'	$= -0.951\ Q_4'' + 0.293\ Q_6''$
Q_5'	$= 0.111\ Q_3'' + 0.137\ Q_4'' - 0.892\ Q_5'' + 0.402\ Q_6'' + 0.102\ Q_8''$
Q_6'	$= -0.256\ Q_4 - 0.412\ Q_5 - 0.859\ Q_6 + 0.151\ Q_7$
Q_7'	$= -0.160\ Q_5'' - 0.982\ Q_7''$
Q_8'	$= -0.999\ Q_8''$
Q_9'	$= 0.994\ Q_9'' - 0.110\ Q_{10}''$
Q_{10}'	$= -0.111\ Q_9'' - 0.994\ Q_{10}''$
Q_{11}'	$= 0.129\ Q_{13}'' - 0.139\ Q_{16}'' + 0.101\ Q_{18}'' - 0.355\ Q_{19}'' + 0.451\ Q_{20}'' - 0.116\ Q_{21}'' + 0.479\ Q_{22}'' - 0.532\ Q_{23}'' + 0.290\ Q_{27}''$
Q_{12}'	$= 0.383Q_{11}'' - 0.919Q_{12}''$
Q_{13}'	$= -0.810\ Q_{11}'' - 0.352\ Q_{12}'' - 0.115\ Q_{13}'' + 0.275Q_{14}'' + 0.282Q_{15}'' - 0.113\ Q_{16}'' - 0.139\ Q_{18}''$
Q_{14}'	$= 0.146Q_{11}'' - 0.732\ Q_{13}'' - 0.230\ Q_{14}'' + 0.298Q_{15}'' + 0.104Q_{18}'' + 0.519Q_{35}''$
Q_{15}'	$= 0.177\ Q_{11}'' - 0.261\ Q_{13} + 0.844\ Q_{14}'' - 0.324\ Q_{15}'' + 0.102\ Q_{16}'' - 0.120\ Q_{19}'' + 0.135\ Q_{35}'' - 0.142\ Q_{37}''$
Q_{16}'	$= 0.226\ Q_{11}'' + 0.105\ Q_{12}'' + 0.276\ Q_{13}'' + 0.312\ Q_{14}'' + 0.795\ Q_{15}'' - 0.247\ Q_{17}'' + 0.219Q_{18}''$
Q_{17}'	$= -0.173\ Q_{15}'' - 0.867\ Q_{16}'' - 0.371''\ Q_{17}'' + 0.246\ Q_{23}''$
Q_{18}'	$= -0.133\ Q_{13}'' + 0.266\ Q_{16}'' - 0.762\ Q_{17}'' - 0.547\ Q_{18}'' - 0.123\ Q_{23}''$
Q_{19}'	$= 0.241\ Q_{11}'' + 0.165\ Q_{15}'' - 0.244\ Q_{16}'' + 0.436\ Q_{17}'' - 0.723\ Q_{18}'' - 0.317\ Q_{19}'' - 0.142\ Q_{22}''$
Q_{20}'	$= -0.126\ Q_{11}'' - 0.115\ Q_{14}'' + 0.221\ Q_{18}'' - 0.816\ Q_{19}'' - 0.439\ Q_{20}'' - 0.169\ Q_{26}''$
Q_{21}'	$= 0.108\ Q_{18}'' + 0.329\ Q_{20}'' - 0.801\ Q_{21}'' - 0.461\ Q_{22}''$
Q_{22}'	$= 0.129\ Q_{18}'' - 0.183\ Q_{19}'' + 0.617\ Q_{20}'' + 0.571Q_{21}'' - 0.445\ Q_{22}''$
Q_{23}'	$= 0.120\ Q_{16}'' - 0.147\ Q_{19}'' + 0.290\ Q_{20}'' + 0.544\ Q_{22}'' + 0.541\ Q_{23}'' - 0.127\ Q_{25}'' - 0.507\ Q_{27}''$
Q_{24}'	$= 0.925\ Q_{24}'' + 0.354\ Q_{25}''$
Q_{25}'	$= -0.351\ Q_{24}'' + 0.907\ Q_{25}'' - 0.160\ Q_{26}'' - 0.105\ Q_{27}''$
Q_{26}'	$= -0.127\ Q_{14}'' - 0.106\ Q_{19}'' + 0.183\ Q_{23}'' + 0.138\ Q_{25}'' + 0.916\ Q_{26}'' + 0.220\ Q_{27}''$
Q_{27}'	$= -0.191\ Q_{16}'' - 0.528\ Q_{23}'' + 0.293Q_{26}'' - 0.754\ Q_{27}''$
Q_{28}'	$= -0.989\ Q_{28}''$
Q_{29}'	$= 0.483\ Q_{29}'' + 0.865\ Q_{44}''$
Q_{30}'	$= 0.991Q_{30}'' + 0.118Q_3''$
Q_{31}'	$= -0.136\ Q_{30}'' + 0.981\ Q_{31}''$
Q_{32}'	$= 0.117\ Q_{31}'' + 0.962\ Q_{32}'' + 0.207\ Q_{46}''$
Q_{33}'	$= 0.994\ Q_{33}''$
Q_{34}'	$= -0.999\ Q_{34}''$
Q_{35}'	$= -0.509\ Q_{13}'' + 0.152\ Q_{15}'' - 0.832\ Q_{35}''$
Q_3'	$= -0.999\ Q_{36}''$
Q_3''	$= -0.138\ Q_{14}'' - 0.988\ Q_{37}''$
Q_{38}'	$= 0.986\ Q_{38}''$
Q_{39}'	$= -0.114\ Q_{41}'' - 0.890\ Q_{42}'' + 0.435\ Q_{43}''$
Q_{40}'	$= 0.174\ Q_{29}'' - 0.401\ Q_{39}'' - 0.857\ Q_{40}'' + 0.209Q_{41}''$
Q_{41}'	$= 0.127\ Q_{29}'' + 0.839\ Q_{39}'' - 0.383\ Q_{40}'' - 0.244\ Q_{41}'' - 0.110\ Q_{42}'' - 0.229\ Q_{43}''$
Q_{42}'	$= 0.414\ Q_{29}'' + 0.109\ Q_{38}'' - 0.357\ Q_{41}'' + 0.349Q_{42}'' + 0.535Q_{43}'' - 0.258\ Q_{44}'' + 0.444Q_{45}''$
Q_{43}'	$= 0.406Q_{29}'' + 0.179\ Q_{39}'' + 0.248\ Q_{40}'' + 0.702\ Q_{41}'' - 0.141\ Q_{42}'' - 0.171\ Q_{43}'' - 0.205\ Q_{44}'' - 0.372\ Q_{45}''$
Q_{44}'	$= 0.208\ Q_{29}''\text{-}0.308\ Q_{39}'' + 0.179\ Q_{40}''\text{-}0.500\ Q_{41}''\text{-}0.218\ Q_{42}''\text{-}0.65\ Q_{43}'' + 0.270\ Q_{45}''$
Q_{45}'	$= 0.574\ Q_{29}''\text{-}0.326\ Q_{44}''\text{-}0.732\ Q_{45}''$
Q_{46}'	$= 0.207\ Q_{32}'' + 0.122\ Q_{45}''\text{-}0.945\ Q_{46}''\text{-}0.115\ Q_{47}''\text{-}0.130\ Q_{48}''$
Q_{47}'	$= 0.139\ Q_{46}''\text{-}0.960\ Q_{47}''\text{-}0.161\ Q_{48}''$
Q_{48}'	$= -0.129\ Q_{46}''\text{-}0.215\ Q_{47}'' + 0.944\ Q_{48}''\text{-}0.139\ Q_{50}''$
Q_{49}'	$= -0.111\ Q_{47}''\text{-}0.204\ Q_{48}''\text{-}0.760\ Q_{49}'' - 0.562\ Q_{50}'' - 0.213\ Q_{51}''$
Q_{50}'	$= -0.610\ Q_{49}'' + 0.732\ Q_{50}'' + 0.282\ Q_{51}''$
Q_{51}'	$= 0.360\ Q_{50}'' - 0.932\ Q_{51}''$

[a] Only terms with coefficients greater than 0.10 are shown.

prominently on any vibronic band other than the electronic origin. This behavior is in contrast to the spectral feature of a partly similar system *p*-aminotoluene, studied by Yan and Spangler about a decade ago. In this case, the rotor motion efficiently couples with the amine inversion.[7] As a result, the overtone of the amine inversion appears as a multiplet band in the $S_1 \leftarrow S_0$ excitation spectrum. In the present system, in addition to the methyl torsion, the other two large amplitude vibrations are phenyl-vinyl torsion and vinyl bending. Hollas et al. estimated that the excited state (S_1) frequencies of the latter two modes in styrene are 186 and 99 cm^{-1},[35] respectively. However, the vibronic signatures of the coupling of the rotor with these large amplitude modes do not show up in the FE spectrum (Figure 3a) with sufficient Franck−Condon intensity.

C. Dispersed Fluorescence Spectra. *C.1. Fluorescence Spectrum of the 0_0^0 Band.* The resolved fluorescence spectrum following excitation of the 0_0^0 band of *p*-VT is presented in Figure 4. Vibronic assignments are suggested with the aid of ground-state harmonic vibrational frequencies of the normal modes predicted by the DFT and CASSCF calculations. The assignments are presented in Table 5. It is seen that the Franck−Condon active major vibronic features in the spectrum correspond only to the in-plane modes. The spectrum also shows the overtones and totally symmetric combinations of a few out-

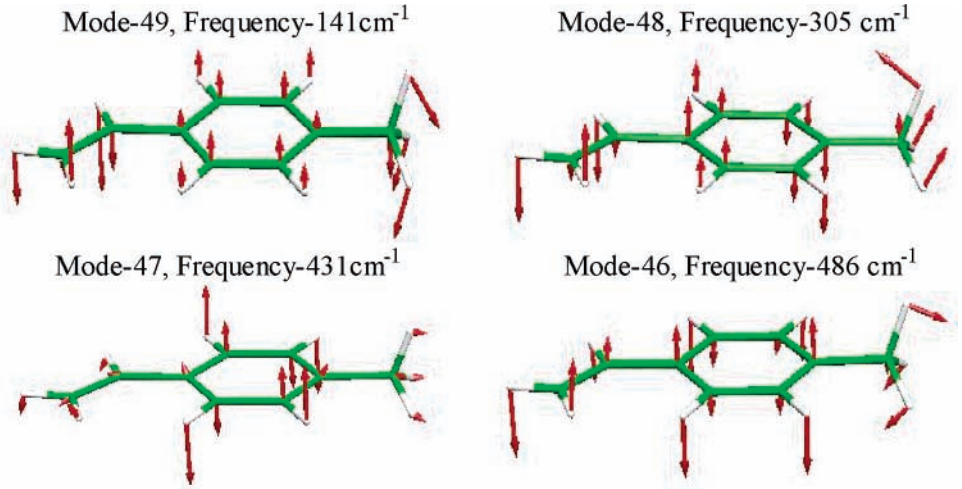

Figure 2. Atom displacement vectors of the normal mode numbers 49, 48, 47, and 46 of *p*-VT calculated at the CASSCF/6-31G* level of theory.

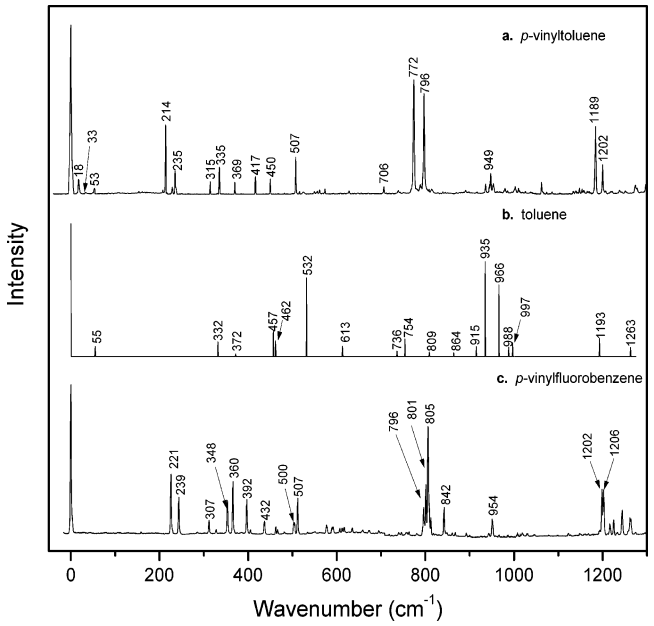

Figure 3. LIF excitation spectra of (a) *p*-VT, (b) T (stick spectral representation) reproduced from ref 25, and (c) *p*-VFB.

of-plane vibrations. However, in general, their intensities are relatively weaker except for those of the low-frequency bands near the origin at 18, 53, 84, and 173 cm^{-1}. The first two of this low-frequency series belong to the methyl torsional progression and they can be assigned as $(51)^{1e}_{2e}$ and $(51)^{0a1}_{3a1}$. The band at 84 cm^{-1} can be assigned to the overtone of the phenyl-vinyl torsion $(50)^0_2$ and the 173 cm^{-1} band to the combination of $(50)^0_1$ and the out-of-plane bending of the vinyl group $(49)^0_1$. In case of *p*-VFB these two transitions appear at 82 and 178 cm^{-1}, respectively.

The validity of approximate C_s point group symmetry representation of the molecule is justified observing the mutually exclusive vibronic spectral characteristics in the emission spectrum of the S_1 origin band and the vibrational band structures in the gas-phase IR absorption spectrum.[32] Figure 5 shows such a comparison in the spectral range of 650 to 1900 cm^{-1}. The frequencies and relative intensities of the IR bands are presented here in stick spectral format. In the emission spectrum, the intense band at 822 cm^{-1} corresponds to the in-plane ring breathing mode. On the other hand, the adjacent bands in the IR absorption spectrum at 829 and 902 cm^{-1} correspond to the fundamental transitions of the out-of-plane ring C−H vibration (mode 43) and out-of-plane vinyl C−H vibrations (mode 41). The DFT predicted frequencies for the latter two modes are 826 and 895 cm^{-1}, respectively. The assignments are justified on the basis of their predicted IR intensities.

A notable feature of the fluorescence spectrum is that the low-frequency bands (18 and 84 cm^{-1}), which have been assigned to methyl torsion and phenyl-vinyl torsion, appear repeatedly as combinations with all the major vibronic bands through out the spectrum. However, as pointed out before, such transitions are absent in the excitation spectrum. This asymmetry indicates that these modes could be mixed with other modes in the excited state as predicted in our theoretical calculation. To verify this possibility we have measured the fluorescence spectra following SVL excitations of all the major vibronic bands, and the results are presented below.

C.2. Fluorescence Spectra of the Vibronic Bands. Figure 6 shows the dispersed fluorescence spectra recorded following excitations of the $0^0_0 + 214$ and $0^0_0 + 235$ cm^{-1} bands. In the first case (Figure 6b), the emission spectrum shows very regular behavior. The first strong band at 209 cm^{-1} displacement from the excitation frequency corresponds to the fundamental of the in-plane bending of the vinyl group in S_0, and the transition is assigned as $(34)^1_1$. All of the other bands in the spectrum can be assigned by adding 209 cm^{-1} to the vibronic frequencies of the emission spectrum of the 0^0_0 band. Therefore, $0^0_0 + 214$ cm^{-1} band in the FE spectrum can be assigned as $(34)^1_0$ transition.

In contrast, the emission spectrum of the $0^0_0 + 235$ cm^{-1} band (Figure 6c) is quite atypical. The most intense band in the spectrum at 267 cm^{-1} displacement from the excitation position behaves as sequence origin. The built up of the 0^0_0-excited emission spectral structure on it has been denoted by dotted lines. In Figure 6a (0^0_0-excited emission spectrum), the 267 cm^{-1} band appears very weakly and it has been assigned as the overtone of the out-of-plane vinyl bending, $(49)^0_2$ (Table 5). Therefore, the band at $0^0_0 + 235$ cm^{-1} in the FE spectrum can be assigned as $(49)^2_0$. However, there are distinct cross-sequence bands in Figure 6c at 84, 136, and 190 cm^{-1} displacements. These three bands can be assigned as $(49)^0_2(50)^0_2$, $(49)^0_2(50)^0_2(51)^{0a1}_{3a1}$, and $(49)^2_1(50)^0_1(51)^{1e}_{2e}$ transitions, respectively. Such spectral features clearly show that on electronic excitation the methyl torsion (51) and vinyl torsion (50) modes undergo mixing with vinyl bending (49) mode and these observations are nicely corroborated with the predictions of the theoretical calculations presented in Table 3.

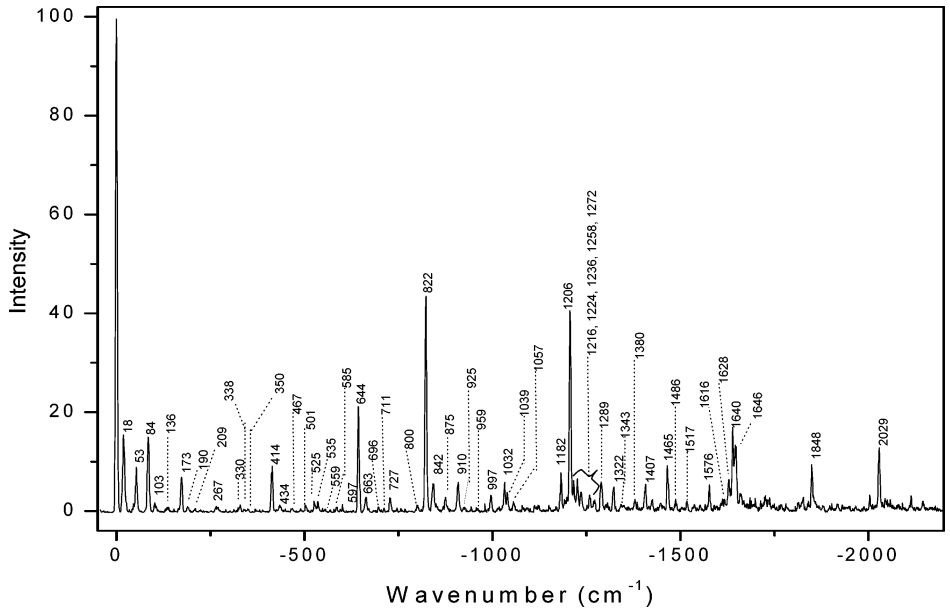

Figure 4. Resolved fluorescence spectrum of *p*-VT recorded following excitation of the $S_1 \leftarrow S_0$ electronic origin band (0_0^0).

Figure 7a−d shows the SVL fluorescence spectra measured following excitations of the $0_0^0 + 335$, $0_0^0 + 417$, $0_0^0 + 450$, and $0_0^0 + 507$ cm^{-1} bands. In Figure 7a, the emission band at 350 cm^{-1} can be recognized as the sequence origin band, and on the basis of the assignment of a band at the same frequency in the emission spectrum of the 0_0^0 band (Table 5), we assign the sequence origin here as $(49)_2^2(51)_2^2$ transition. In addition, there are distinct cross-sequence bands at 84, 136, 173, 190, 330, and 535 cm^{-1}, and all of these bands show up weakly in the emission spectrum of the electronic origin band (0_0^0). The appearance of the cross-sequence band at 535 cm^{-1} is interesting. In the S_0 surface, the frequency corresponds to the combination of the vinyl torsion with the out-of-plane ring puckering $(46)_1(50)_1$ (Table 5). Therefore, the cross-sequence transition at this frequency clearly demonstrates that electronic excitation leads to mixing of the methyl and vinyl torsions with the out-of-plane ring puckering motion.

On the other hand, the features of the emission spectrum of the $0_0^0 + 417$ cm^{-1} band (Figure 7b) are such that no specific band can be assigned as a sequence origin. This implies that the 417 cm^{-1} band in the FE spectrum is the effect of extensive mixing of many of the ground-state vibrations. The two prominent bands at 695 and 800 cm^{-1} (Figure 7b) correspond to the $(30)_1^0(51)_{3a1}^{0a1}$ and $(47)_2^0$ transitions of the 0_0^0-excited emission spectrum. In S_0, the mode 30 corresponds to the in-plane ring distortion of frequency 644 cm^{-1}, and the mode 47 corresponds to the out-of-plane ring puckering vibration. Thus, the cross-sequence bands at 695 and 800 cm^{-1} in Figure 7b imply that in the excited state the in-plane and out-of-plane modes undergo partial mixing involving the methyl torsion. Likewise, the emission spectrum measured following excitation of the $0_0^0 + 450$ cm^{-1} band (Figure 7c) exhibits extensive cross-sequence transitions. Here, the first band at 585 cm^{-1} correspond to the overtone of the ring puckering transition $(48)_2^0$ in the S_0 surface (Table 5). Appearance of this transition along with those of the 695 and 800 cm^{-1} bands in this emission spectrum further indicate the signature of mixing of the in-plane and out-of-plane modes involving the methyl torsion.

In contrast, the spectral features in Figure 7d are quite regular. The sequence band at 525 cm^{-1} in this spectrum corresponds to the fundamental of an in-plane ring bending mode. Although the excitation energy in this case is relatively higher ($0_0^0 + 507$ cm^{-1}), the pattern of the atomic motions of the mode remain undistorted on electronic excitation, and the same has been predicted also for a few other cases by the theoretical calculation.

Figure 8 shows the general features of the evolution of the fluorescence spectra of the molecule as a function of excess vibronic excitation energy. Sharp vibronic structures in the fluorescence spectra are observed for excitations up to $0_0^0 + 507$ cm^{-1} band. On the other hand, only broad and featureless emission spectra are observed for vibronic excitation energies beyond 1200 cm^{-1}. In the intermediate range of vibronic excitations, e.g., $0_0^0 + 772$ and $0_0^0 + 796$ cm^{-1}, sharp spectral features are observed over broad emission profiles. The broad features are an indication of intramolecular vibrational redistribution (IVR) in the excited state. To find the role of the methyl torsion in the IVR process depicted here, the vibronic energy dependent emission spectra of *p*-VFB, which does not have a rotor group, have been measured and presented in the figure for comparison. The latter molecule exhibits only sharp emission spectra following excitations in the vibronic energy range considered here.

D. Role of the Vinyl Group in S_1 Dynamics of *p*-VT. To understand the role of the *p*-vinyl group in excess vibronic energy dependent emission spectral behavior of the molecule presented here, it is instructive to compare the emission spectral features of toluene for different vibronic excitations of similar excess energies. The resolved emission spectra of the latter in a supersonic free jet expansion following excitations of the $6b_0^1$, 12_0^1, and $18a_0^1$ bands, which are, respectively at 530, 933, and 965 cm^{-1} above S_1 electronic origin, were measured earlier by Hopkins et al.[36] In all three cases, the emission spectra display only regular features of SVL excitations, and no unusual characteristics of the excited-state level mixing are displayed in the emission spectra. More recently, Hickman et al. have measured the DF spectra following excitations of all of the vibronic bands in the energy range of 0−1500 cm^{-1} in S_1, and the gross observations are similar to those of Hopkins et al. However, excitations of a few weaker bands of vibronic energy more than 1000 cm^{-1} result in emission spectra containing sharp structures over small backgrounds, which start at displacements of ∼1000 cm^{-1} from the excitation frequencies. Thus, it appears

TABLE 5: Vibronic Frequencies and Their Assignments in the Resolved Fluorescence Spectrum of *p*-VT Measured by Exciting the 0_0^0 Band[a]

observed freq. (cm^{-1})	relative intensity	assignment	calc. S_0 freq. (fundam.) DFT[c]	calc. S_0 freq. (fundam.) CASSCF[d]
0[b]	100	0_0^0		
18	15	$(51)_{2e}^{1e}$	20	14
53	11	$(51)_{3a1}^{0a1}$		
84	15	$(50)_2^0$	70	11
103	2	$(50)_2^0(51)_{2e}^{1e}$		
136	1	$(50)_2^0(51)_{3a1}^{0a1}$		
173	7	$(49)_1^0(50)_1^0$	146	132
190	1	$(49)_1^0(50)_1^0(51)_{2e}^{1e}$		
209	0.5	$(34)_1^0$	211	207
267	1	$(49)_2^0$		
330	2	$(33)_1^0$		
350	0.8	$(49)_2^0(50)_2^0$	340	343
414	10	$(32)_1^0$		
434	1.5	$(32)_1^0(51)_{2e}^{1e}$	414	414
467	0.8	$(32)_1^0(51)_{3a1}^{0a1}$		
503	2	$(32)_1^0(50)_2^0$		
525	2.5	$(31)_1^0$	525	529
535	2.5	$(46)_1^0(50)_1^0$		
585	1	$(48)_2^0$	298	287
644	22	$(30)_1^0$	643	650
663	3	$(30)_1^0(51)_{2e}^{1e}$		
695	0.8	$(30)_1^0(51)_{3a1}^{0a1}$		
727	3	$(30)_1^0(50)_2^0$		
800	2	$(47)_2^0$	410	405
822	44	$(28)_1^0$	818	817
842	6	$(28)_1^0(51)_{2e}^{1e}$		
875	3	$(28)_1^0(51)_{3a1}^{0a1}$		
910	6	$(28)_1^0(50)_2^0$		
997	3	$(28)_1^0(49)_1^0(50)_1^0$		
1032	6	$(26)_1^0$	1014	1037
1039	4	$(25)_1^0$	1036	1063
1057	2	$(24)_1^0$	1043	1078
1182	8	$(23)_1^0$	1123	1116
1206	41	$(22)_1^0$	1207	1193
1216	6	$(21)_1^0$	1186	1218
1224	7	$(22)_1^0(51)_{2e}^{1e}$		
1236	4	$(20)_1^0$	1296	1227
1258	3	$(22)_1^0(51)_{3a1}^{0a1}$		
1272	2	$(19)_1^0$	1216	1254
1289	6	$(22)_1^0(50)_2^0$		
1322	5	$(18)_1^0$, $(17)_1^0$	1313, 1329	1340, 1371
1407	5.5	$(16)_1^0$	1412	1445
1465	9	$(22)_1^0(30)_1^0$		
1576	5	$(13)_1^0$	1580	1605
1616	1	$(12)_1^0$	1625	1659
1628	6	$(22)_1^0(32)_1^0$		
1640	17	$(32)_2^0$		
1646	13	$(11)_1^0$	1654	1676
1848	10	$(12)_1^0(30)_1^0$		
2029	13	$(12)_1^0(28)_1^0$		

[a] Ground-state frequencies calculated by the DFT and CASSCF theories corresponding to the observed fundamentals are presented for comparison. [b] Relative to the $S_1 \leftarrow S_0$ origin transition at 34 297 cm^{-1}. [c] 6-311G** basis set was used. A uniform scaling factor of 0.98 has been used. [d] 6-31G** basis set was used. A uniform scaling factor of 0.94 has been used.

that the dramatically different excess vibronic energy dependent fluorescence spectral behavior of *p*-VT shown in Figure 8 is promoted by the para vinyl group.

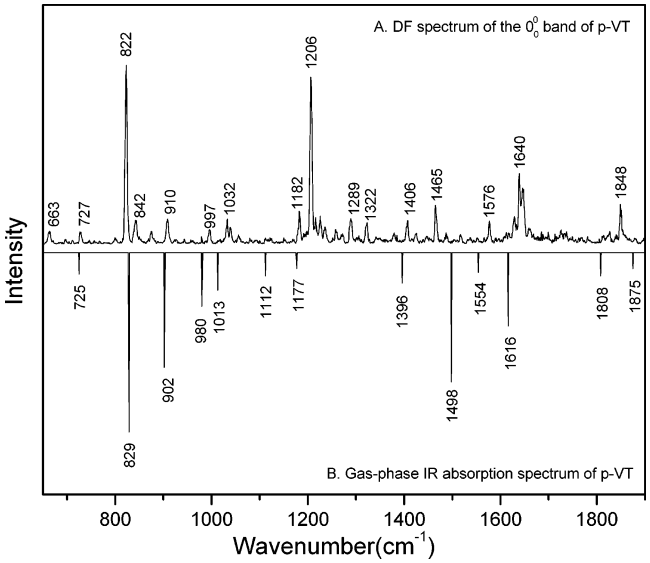

Figure 5. Comparison between the resolved fluorescence spectrum of the 0_0^0 band and the gas-phase IR absorption spectrum (stick spectral format) of *p*-VT. The latter has been reproduced from the ref 32.

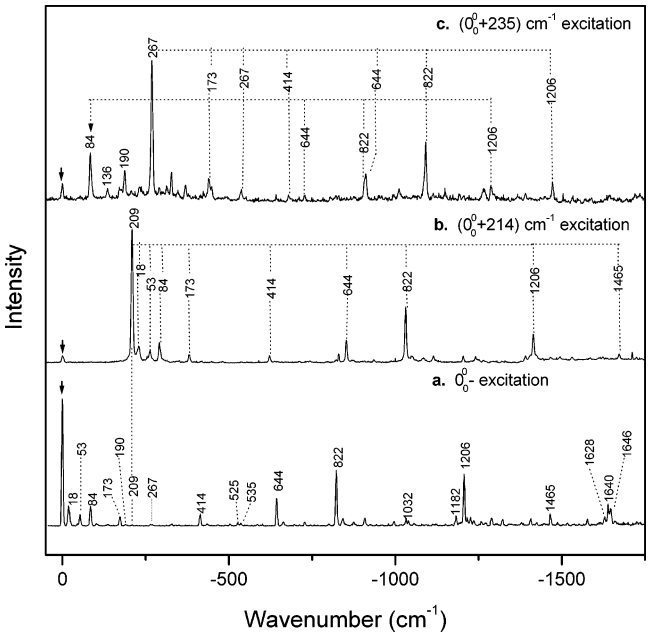

Figure 6. Resolved fluorescence spectra following SVL excitations of the (b) $0_0^0 + 214$ and (c) $0_0^0 + 235$ cm^{-1} bands of *p*-VT. The emission spectrum of the (a) 0_0^0 band is again presented here to make a comparison.

Recently Borst et al.[13] have proposed a mechanism to explain the IVR acceleration by the methyl group in the excited state. Analyzing the rotationally resolved electronic spectra of toluene, the authors suggested that, below the torsional energy barrier, the methyl group executes a precessional motion as it moves along the torsional coordinate. Vibronic excitations beyond the torsional barrier quench the precessional motion, but the ring undergoes larger distortions with internal rotation of the methyl group. This feature of the internal rotational motion in the excited state was suggested as a facile route to IVR. The conclusions of the authors are consistent with the earlier suggestions that level mixing in *p*-FT might be related to excitations of the higher internal rotational levels.[1,4]

Hollas et al. estimated the methyl torsion potential parameters of *p*-VT in the S_0 and S_1 states by analyzing the low-frequency

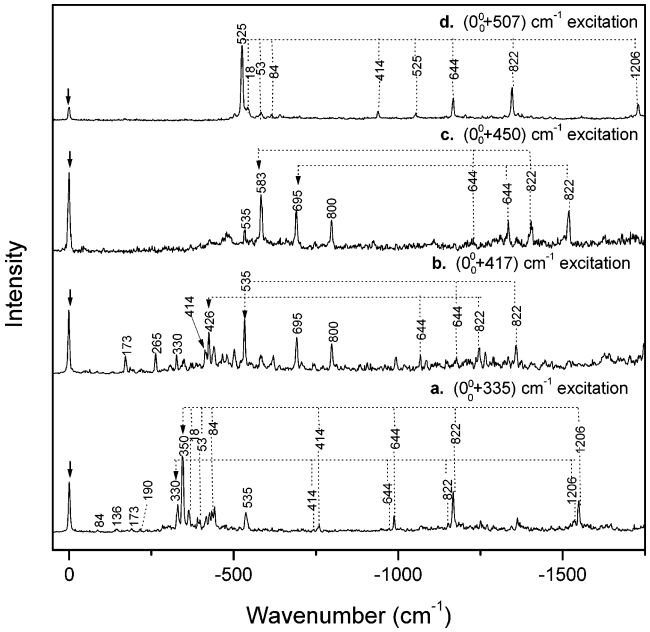

Figure 7. Resolved fluorescence spectra following SVL excitations of the (a) $0_0^0 + 335$, (b) $0_0^0 + 417$, (c) $0_0^0 + 450$, and (d) $0_0^0 + 507$ cm^{-1} bands of *p*-VT.

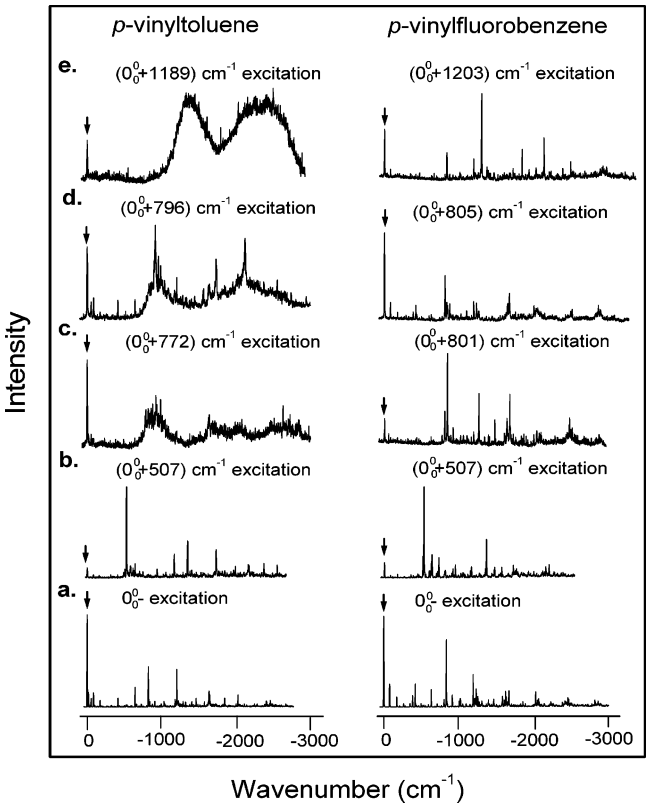

Figure 8. Comparison of the dispersed fluorescence spectra of p-VT and p-VFB in a supersonic jet expansion following excitations of different vibronic bands of comparable energies. All the spectra are recorded at a spectral resolution of 7 cm^{-1}. Excitation positions are denoted by inverted arrows.

vibronic band structures in the fluorescence excitation and resolved emission spectra of the 0_0^0 band.[37] The measured V_6 values are -17 ± 1 and -17 ± 5 cm^{-1} in S_0 and S_1, respectively. In both of the electronic states, the orientation of the methyl group is suggested to be staggered with respect to the plane of the aromatic ring and which are consistent with the predictions of the theoretical results presented in this work. According to these data, the excited-state torsional barrier of *p*-VT is almost half of those estimated for toluene ($V_6' = -26.376$ cm^{-1})[13] and *p*-fluorotoluene ($V_6' = -33.00$ cm^{-1}).[28] Therefore, it appears that the para vinyl substitution facilitates the torsional motion of methyl group, and it could be an important contributing factor to the dynamics of the molecule in the excited state. Because of the lower barrier, the rotor mode can easily be excited to the levels beyond the barrier height through intramolecular vibrational energy transfer from the other excited modes, and according to the model of Borst et al. this may cause larger distortions of the aromatic ring and facilitate the IVR.

The dispersed fluorescence spectral data that we have presented in this study have revealed clearly that the torsional motion of the vinyl group promotes Duschinsky mixing in S_1 involving both the methyl torsion and ring modes. In a number of recent investigations, it has been proposed that such vibrational mode mixing in the excited electronic states can profoundly affect the nonradiative relaxation rates.[38] The comparisons of the dispersed fluorescence spectral patterns following SVL excitations of *p*-VT and *p*-VFB, as presented in Figure 8, reveal that, although the Franck−Condon active vibronic band structures in their FE spectra look similar (Figure 3), the descriptions of their excited-state vibrations in terms of atomic displacements must be very different. Likewise, the background levels to which the excitation energy from the Franck−Condon levels flow are also likely to be different in the two molecules, and the rotor mode of the methyl group could play a crucial role in determining the characteristics of the background levels. Abel and co-workers[19,20] embraced a similar model to interpret their observations in real-time probing of the rotor-induced IVR in toluene in the ground electronic state. Following femtosecond excitation around the two quanta region of the C−H stretch vibration (1.7 μm) of benzene and toluene vapors, a characteristic rise, which has a faster and a slower components, was identified in the transient UV absorptions and that was interpreted as due to IVR in two steps. The IVR acceleration by the methyl group was manifested in slower component, which for toluene was 5−6 times faster than benzene.

A hyperconjugation model was invoked by Yan and Spangler to explain the spectral features of coupling of the methyl torsion with the amine inversion in *p*-aminotoluene (*p*-AT).[7] In the excited state, the amino group is relatively coplanar with the aromatic ring, and the lone pair electrons of the former are shared with the aromatic π system. As a result, the inversion of the amine group can induce oscillation in the aromatic π electrons. It was proposed that the charge oscillation in the ring can be propagated to the methyl group through hyperconjugation. In the present system, the vinyl group is coplanar with the aromatic ring in both of the electronic states. In the excited state, the vinyl π electrons are shared with the aromatic ring and this is reflected in enhanced torsional frequency of the group compared to that in the ground state. Therefore, in principle, such sharing of electrons between the vinyl and phenyl groups can be extended to the methyl group through hyperconjugation. However, unlike *p*-AT, direct spectral signatures of coupling of the rotor motion with other modes involving the vinyl torsion are not directly manifested in the FE spectrum of *p*-VT. Thus, the coupled levels are Franck−Condon inactive. Our DF spectral data reveals that such states can be reached through the mechanism of mode mixing.

Acknowledgment. The authors gratefully acknowledge the financial support received from the Department of Science and

Technology (DST), Govt. of India, to carry out the research. P.B. thanks the CSIR for a Junior Research Fellowship under the Project, No. 01(1751)/02/EMR-II, and S.S.P. thanks the University Grant Commission, Govt. of India, for a Senior Research Fellowship.

References and Notes

(1) Parmenter, C. S.; Stone, B. M. *J. Chem. Phys.* **1986**, *84*, 4710.
(2) Moss, D. B.; Parmenter, C. S.; Ewing, G. E. *J. Chem. Phys.* **1987**, *86*, 51.
(3) Moss, D. B.; Parmenter, C. S. *J. Chem. Phys.* **1993**, *98*, 6897.
(4) Baskin, J. S.; Rose, T. S.; Zewail, A. H. *J. Chem. Phys.* **1988**, *88*, 1458.
(5) Alves, A. C. P.; Hollas, J. M.; Musa, H.; Ridley, T. *J. Mol. Spectrosc.* **1985**, *109*, 99.
(6) Redington, R. L.; Chen, Y.; Scherer, G. J.; Field, R. W. *J. Chem. Phys.* **1988**, *88*, 627.
(7) Yan, S.; Spangler, L. H. *J. Chem. Phys.* **1992**, *96*, 4106.
(8) Gambogi, J. E.; L'Esperance, R. P.; Lehmann, K. K.; Pate, B. H.; Scoles, G. *J. Chem. Phys.* **1993**, *98*, 1116.
(9) Perry, D. S.; Bethardy, G. A.; Wang, X. *Ber. Bunsen-Ges., Phys. Chem.* **1995**, *99*, 530.
(10) Spangler, L. H.; Pratt, D. W. In *Jet Spectroscopy and Molecular Dynamics*; Hollas, J. M., Phillips, D., Eds.; Chapman & Hall: London, 1995; p 366.
(11) Nishi, K.; Sekiya, H.; Kawakami, H.; Mori, A.; Nishimura, Y. *J. Chem. Phys.* **1999**, *111*, 3961.
(12) Nishi, K.; Sekiya, H.; Mochida, T.; Sugawara, T.; Nishimura, Y. *J. Chem. Phys.* **2000**, *112*, 5002.
(13) Borst, D. R.; Pratt, D. W. *J. Chem. Phys.* **2000**, *113*, 3658.
(14) Cavagnat, D.; Lespade, L. *J. Chem. Phys.* **2001**, *114*, 6030.
(15) Pinsker, M.; Friedrich, J. *J. Chem. Phys.* **2002**, *117*, 4639.
(16) Davies, J. A.; Reid, K. L.; Towrie, M.; Matousek, P. *J. Chem. Phys.* **2002**, *117*, 9099.
(17) Vendrell, O.; Moreno, M.; Lluch, J. M. *J. Chem. Phys.* **2002**, *117*, 7525.
(18) Bellm, S. M.; Whiteside, P. T.; Reid, K. L. *J. Phys. Chem. A* **2003**, *107*, 7373.
(19) Assmann, J.; Benten, R. v.; Charvat, A.; Abel, B. *J. Phys. Chem. A* **2003**, *107*, 1904.
(20) Benten, R. v.; Link, O.; Abel, B.; Schwarzer, D. *J. Phys. Chem. A* **2004**, *108*, 363.
(21) Chou, Y.-C.; Chen, I.-C.; Hougen, J. T. *J. Chem. Phys.* **2004**, *120*, 2255.
(22) Panja, S. S.; Chakraborty, T. *J. Phys. Chem. A* **2003**, *107*, 10984.
(23) Panja, S. S.; Chakraborty, T. *J. Chem. Phys.* **2003**, *119*, 9486.
(24) Georgiev, S.; Neusser, H. J.; Chakraborty, T. *J. Chem. Phys.* **2004**, *120*, 8015.
(25) Hickman, C. G.; Gascooke, J. R.; Lawrence, W. D. *J. Chem. Phys* **1996**, *104*, 4887.
(26) Frisch, M. J.; Trucks, G. W.; Schlegel, H. B.; Scuseria, G. E.; Robb, M. A.; Cheeseman, J. R.; Zakrzewski, V. G.; Montgomery, J. A., Jr.; Stratmann, R. E.; Burant, J. C.; Dapprich, S.; Millam, J. M.; Daniels, A. D.; Kudin, K. N.; Strain, M. C.; Farkas, O.; Tomasi, J.; Barone, V.; Cossi, M.; Cammi, R.; Mennucci, B.; Pomelli, C.; Adamo, C.; Clifford, S.; Ochterski, J.; Petersson, G. A.; Ayala, P. Y.; Cui, Q.; Morokuma, K.; Malick, D. K.; Rabuck, A. D.; Raghavachari, K.; Foresman, J. B.; Cioslowski, J.; Ortiz, J. V.; Stefanov, B. B.; Liu, G.; Liashenko, A.; Piskorz, P.; Komaromi, I.; Gomperts, R.; Martin, R. L.; Fox, D. J.; Keith, T.; Al-Laham, M. A.; Peng, C. Y.; Nanayakkara, A.; Gonzalez, C.; Challacombe, M.; Gill, P. M. W.; Johnson, B. G.; Chen, W.; Wong, M. W.; Andres, J. L.; Head-Gordon, M.; Replogle, E. S.; Pople, J. A. *Gaussian 98*, revision A.11.1; Gaussian, Inc.: Pittsburgh, PA, 1998.
(27) East, A. L. L.; Liu, H.; Lim. E. C.; Jensen, P.; Dechene, I.; Zgierski, M. Z.; Siebrand, W.; Bunker, P. R. *J. Chem. Phys.* **2000**, *112*, 167.
(28) Zhao, Z.-Q.; Parmenter, C. S.; Moss, D. B.; Bradley, A. J.; Knight, A. E. W.; Owens, K. G. *J. Chem. Phys.* **1992**, *96*, 6362.
(29) Hollas, J. M.; Khalilipour, E.; Thakur, S. N. *J. Mol. Spectrosc.* **1978**, *73*, 240.
(30) Syage, J. A.; Al Adel, F.; Zewail, A. H. *Chem. Phys. Lett.* **1983**, *103*, 15.
(31) Hemley, R. J.; Leopold, D. G.; Vaida, V.; Karplus, M. *J. Chem. Phys.* **1985**, *82*, 5379.
(32) NIST Database, http://webbook.nist.gov
(33) Hollas, J. M.; Hussein, M. Z. B. *J. Mol. Spectrosc.* **1991**, *145*, 89.
(34) Okuyama, K.; Mikami, N.; Ito, M *J. Phys. Chem.* **1985**, *89*, 5617.
(35) Hollas, J. M.; Ridley, T. *J. Mol. Spectrosc.* **1981**, *89*, 232.
(36) Hopkins, J. B.; Powers, D. E.; Mukamel, S.; Smalley R. E. *J. Chem. Phys.* **1980**, *72*, 5049.
(37) Hollas, J. M.; Taday, P. F. *J. Chem. Soc., Faraday Trans.* **1990**, *86*, 217.
(38) Mebel, A. M.; Hayashi, M.; Liang, K. K.; Lin, S. H. *J. Phys. Chem. A* **1999**, *103*, 10674.